

Type III pleuropulmonary blastoma: A case report

SHUAI LUO, XIAOXUE TIAN, TING XU and JINJING WANG

Department of Pathology, Affiliated Hospital of Zunyi Medical University, Zunyi, Guizhou 563000, P.R. China

Received September 26, 2024; Accepted December 11, 2024

DOI: 10.3892/ol.2025.14864

Abstract. Pleuropulmonary blastoma (PPB) is an uncommon malignant neoplasm occurring in infants. The disease is intimately linked to mutations in the Dcr-1 homolog and ribonuclease type III (DICER1) genes. Imaging techniques are crucial for diagnosing PPB, yet distinguishing PPB from other pulmonary masses proves challenging. Early detection of PPB is problematic, and it is often diagnosed at an advanced pathological stage with a poor prognosis. The present report discusses a PPB case and evaluates its clinical manifestations, imaging characteristics, pathological features and molecular genetic changes. The patient was a 3-year-old female who presented to Affiliated Hospital of Zunyi Medical University (Zunyi, China) with an unexplained cough. Chest computed tomography revealed a mass in the right thoracic cavity, which was identified as a neoplastic lesion and considered a potential PPB. Surgical intervention was performed. The postoperative pathological examination confirmed PPB (type III) with rhabdomyomatous and chondroid differentiation. After surgery, the patient was treated with regular chemotherapy and at follow-up was doing well without recurrence. In conclusion, PPB represents a rare pathological diagnosis. The present report highlights the significance of noting clinical symptoms in infants, promptly performing pulmonary imaging and pathological examinations, and performing genetic testing when required. Furthermore, long-term surveillance of families with DICER1 syndrome is vital for infants diagnosed with PPB.

Introduction

Pleuropulmonary blastoma (PPB) predominantly manifests in infants, particularly those <6 years old (1). According to the data of the International PPB registry, the incidence of

PPB is 0.35-0.65/100 000 (2). According to the pathological findings (3), PPB can be divided into three types: Type I is cystic without solid component; Type II is a cystic-solid mass; and type III is a complete solid mass with liquefaction and necrosis. The prognosis of PPB is significantly correlated with the pathological type and stage of the tumor. Type I PPB can progress to Type II and III, and the prognosis of type I PPB is significantly more favorable than that of Type II and III PPB, since type II and III PPB often have recurrence and distant metastasis. According to a study (4), the 5-year survival rate of patients with Type I PPB is 82%, and that of Type II and III PPB is 71 and 53%, respectively. Therefore, early diagnosis of PPB is necessary, which is of great significance to improve the survival rate of patients.

The primary clinical manifestations are respiratory symptoms, including cough, fever, dyspnea and respiratory distress. Imaging examinations can enable in the diagnostic process; however, pathological examination remains the 'gold standard' for the diagnosis of PPB. The pathological classification of PPB is highly linked to both the treatment approach and the prognosis of the patient. Therefore, accurate pathological classification is crucial. Type I and Type Ir PPB (also known as degenerative or static PPB, it is so named since only well-differentiated fibers and cartilage can be seen in the tumor capsule wall and the lack of primitive childish embryonic components) are primarily managed with surgical intervention, supplemented by radiotherapy if required, whereas Types II and III necessitate chemotherapy following surgical resection. The exact pathogenesis of PPB remains unknown (5).

The present report describes the case of PPB and analyses its clinical manifestations, imaging features, pathological features and molecular genetic changes to improve the understanding of this disease.

Case report

A 3-year-old female patient was admitted to the Affiliated Hospital of Zunyi Medical University (Zunyi, China) in May 2023 for further evaluation after presenting with a 2-month history of cough without obvious inducement and without symptoms including sputum, fever, chills, shortness of breath, dyspnea, abdominal pain, abdominal distension, nausea, vomiting, urinary frequency, and urgency. The symptoms had not markedly improved after oral anti-inflammatory treatment. A chest X-ray revealed bronchitis and a mass in the right thoracic cavity (data not shown), prompting a recommendation

Correspondence to: Dr Jinjing Wang, Department of Pathology, Affiliated Hospital of Zunyi Medical University, 149 Dalian Road, Zunyi, Guizhou 563003, P.R. China
E-mail: jinjingwangls@163.com

Abbreviations: PPB, pleuropulmonary blastoma; DICER1, Dcr-1 homolog and ribonuclease type III; CT, computed tomography

Key words: diagnosis, infant, imaging, pleuropulmonary blastoma, treatment

for a contrast-enhanced chest computed tomography (CT) scan. Physical examination showed a good mental state, no evident three concave signs, a stable and regular breathing rhythm, symmetrical thorax bilaterally, no pleural friction rub and no subcutaneous crepitus. The right lung exhibited hyper-resonance with distinct fine moist rales. A chest CT plain scan and enhanced scan revealed a mass measuring $\sim 85 \times 74 \times 68$ mm in the right lower thoracic cavity with uneven density, clear boundaries, and significant heterogeneous enhancement on the contrast-enhanced scan (Figs. 1 and 2). Multiple tortuous vascular shadows were noted within the mass. The right lower lobe was compressed, and flaky increased density shadows were observed in the right middle and lower lobes. The mediastinum remained centered, with no enlarged lymph nodes in the mediastinum or bilateral pulmonary hila. The size and morphology of the heart appeared normal. These findings indicated a space-occupying lesion in the right thoracic cavity, which was considered a neoplastic lesion likely representing PPB.

Following the completion of relevant examinations (including routine blood work, liver function test, coagulation function test, HIV⁺, syphilis⁺ hepatitis C and other infection indicators, stool and urine test, heart color Doppler ultrasound and electrocardiogram) and the exclusion of surgical contraindications, a thoracoscopic right middle and lower lobectomy with thoracic lesion resection was performed. Intraoperative findings revealed firmer lung tissue in the right middle and lower lobes, with the tumor occupying nearly the entire middle and lower lobes, measuring $80 \times 70 \times 60$ mm, with indistinct boundaries and slightly thickened interlobar fissures.

A pathological biopsy examination was performed on the lung tissue specimen, measuring $92 \times 85 \times 76$ mm. Gross examination revealed a mass of fragmented gray-white to gray-brown tissue, $\sim 81 \times 72 \times 58$ mm in size (Fig. 3). The cut surface appeared gray-white and solid, with a delicate cut surface. The boundary between the mass and the surrounding lung tissue was relatively distinct, with certain areas exhibiting tight adhesion to the visceral pleura. The specimens were fixed in 4% neutral formalin at room temperature for 12 h, followed by routine dehydration, paraffin embedding and sectioning at a thickness of 5 μ m. Hematoxylin and eosin staining was then performed at room temperature for 5 min each. Microscopic examination (Leica Biosystems) at low magnification revealed tumor cells diffusely distributed in sheets with high cellular density, and a few glandular-like structures were visible between the spindle-shaped solid sheets of tissue (Fig. 4). At high magnification, the solid part was composed of immature primitive embryonic components (Fig. 5), lacking malignant epithelial elements. In certain areas, embryonal rhabdomyosarcoma (ERMS)-like differentiation (Fig. 6) and immature chondrosarcoma-like differentiation (Fig. 7) were observed. The tumor cells exhibited anaplastic changes, with hyperchromatic enlarged nuclei, an increased nucleo-cytoplasmic ratio, and the presence of tumor giant cells and pathological mitotic figures.

For immunohistochemistry, the specimens were fixed in 10% neutral formalin (12 h) at 28°C., followed by routine dehydration, paraffin embedding and sectioning at a thickness of 3 μ m. Immunohistochemistry using the Envision twostep method was employed to assess the expression of relevant proteins in the tumor tissue. The staining procedures were

performed strictly according to the manufacturer's instructions (all primary antibodies used were rabbit or mouse anti-human monoclonal antibodies, purchased from Fuzhou Maixin Biotechnology Development Co. Ltd., and were used at a working concentration of 1:100). The primary antibodies were added to the sections and incubated overnight (12 h) at 4°C. The sections were then prewarmed at 37°C for 30 min, washed 3 times (5 min/time) with PBS (cat. no. TW-0821), incubated in an oven at 37°C for 15 min with secondary antibody (cat. no. DNS-0811) and washed 3 times (5 min/time) with PBS. DAB color development (cat. no. TT-0801; 1:20 preparation) was performed. Microscopic examination (Leica Biosystems) results demonstrated the following: The tumor cells exhibited positivity for Vimentin (cat. no. RMA0547), CD10 (cat. no. MAB0668) and CD56 (cat. no. MAB0743) (Fig. 8A-C). Desmin, myogenic differentiation 1 (MyoD1) (cat. no. MAB0822) and CD99 (cat. no. MAB0059) were focally or sporadically positive (Fig. 8D-F). Spalt like transcription factor 4 (cat. no. MAB0691) demonstrated focal positivity (Fig. 8G), whilst smooth muscle actin (SMA; cat. no. Kit0006) showed local focal positivity (Fig. 8H). Myogenin (cat. no. MAB0866) exhibited local scattered focal positivity (Fig. 8I). Human Melanoma Black 45 (cat. no. MAB0098) was sporadically positive in certain regions and CD34 (cat. no. Kit0004) displayed local positivity (Fig. S1). CK-Pan (AE1/AE3; cat. no. Kit0009), epithelial membrane antigen (cat. no. Kit0011), thyroid transcription factor-1 (TTF-1; cat. no. MAB0677) and Catenin (cat. no. MAB0754) were positive in the mature epithelium entrapped within the tumor, and signal transducer and activator of transcription 6 (cat. no. MRA0845), anaplastic lymphoma kinase (ALK; cat. no. MAB0848), CD21 (cat. no. MAB0708), Chromogranin A (cat. no. MAB0707), OCT3/4 (cat. no. MAB0874), S-100 (cat. no. Kit0007) and Synaptophysin (cat. no. MAB0742) were all negative (Fig. S2).

Based on the clinical history, pathological morphological characteristics and immunohistochemical results, the diagnosis was as follows: PPB (Type III) of the right middle and lower lobes, accompanied by rhabdomyosarcoma, chondrosarcoma and other differentiation. The tumor involved the visceral pleura, whilst the bronchial and pulmonary stumps were not affected by the tumor.

After surgery, the patient was treated with IVADo (ifosfamide + vincristine + actinomycin D + adriamycin) regimen for 12 courses in Chongqing Children's Hospital (Chongqing, China). IVADo chemotherapy consisted of ifosfamide 3 g/m²/dose IV on days 1 and 2 (6 g/m²/cycle) with MESNA, vincristine 1.5 mg/m² IV on day 1 (maximum 2 mg), actinomycin-D 1.5 mg/m² IV on day 1 (maximum 2 mg) and doxorubicin 30 mg/m²/dose IV on days 1 and 2 (60 mg/m²/cycle) for four 21-day cycles followed by IVA (ifosfamide, vincristine and actinomycin-D) on day 1 for eight 21-day cycles. The patient was reexamined by chest and abdominal imaging every 3 months. At present, the patient has recovered well and has had no recurrence.

Discussion

Characteristics of the disease. Malignant lung tumors in infants are rare, constituting only 0.5-1.0% of primary lung neoplasms at the global level (6). PPB, first characterized in

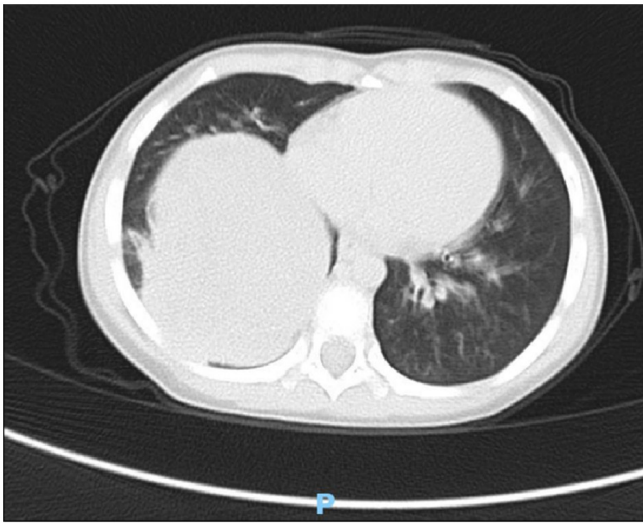


Figure 1. Chest CT plain scan shows a mass of ~85x74x68 mm in size in the lower right chest with uneven density and clear boundaries.

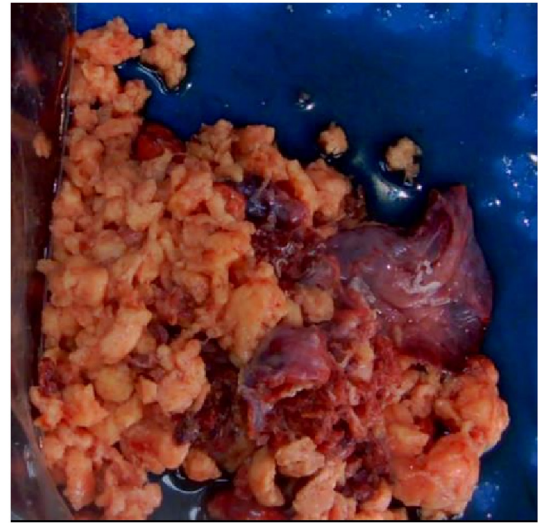


Figure 3. Observation of the lung tissue reveals a mass of fragmented gray-white and gray-brown tissue. The cut surface appears gray and solid with a delicate texture.

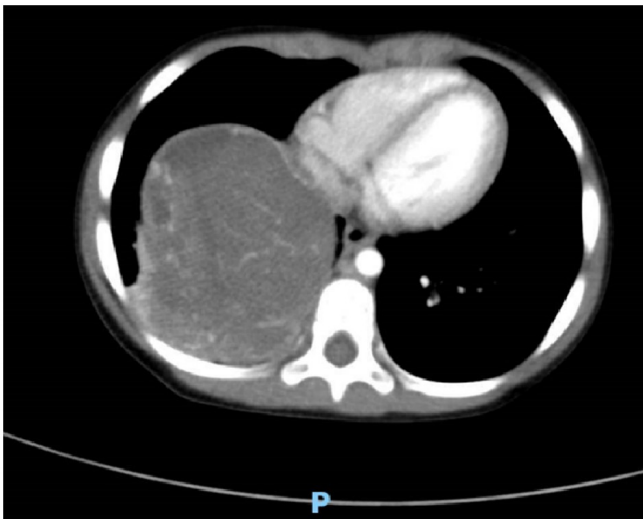


Figure 2. Chest CT enhancement shows uneven and obvious enhancement of the lower right thoracic mass.

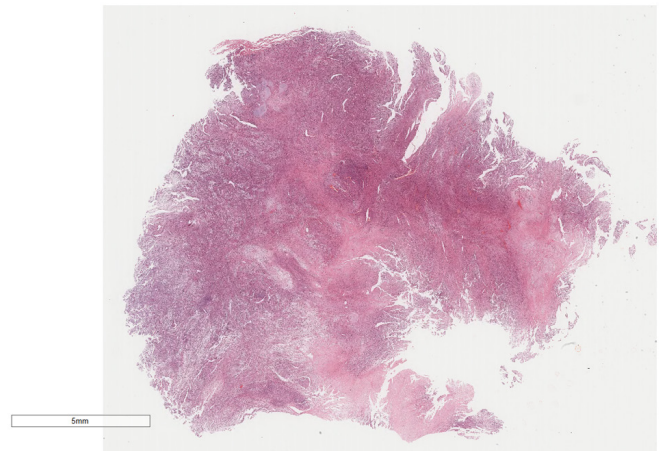


Figure 4. Low-power microscopy reveals that the tumor cells are diffuse and distributed with high cell density (H&E stain; magnification, x10).

1988, is identified as a malignant tumor arising within the pulmonary interstitium of infants and is the most prevalent primary lung tumor in this demographic, typically originating from the lung and/or pleura (7). It predominantly comprises malignant primitive embryonic mesenchymal components along with benign pulmonary epithelial elements. The clinical manifestations of PPB are nonspecific, primarily including respiratory symptoms such as cough, sputum and dyspnea. Consequently, PPB is often missed or misdiagnosed (5). Furthermore, the majority of cases documented in the literature pertain to infants <6 years old (4,8), though instances have been noted in adolescents (9) and even adults (10-12). Moreover, the incidence rate shows no significant difference between sexes. Common metastatic sites encompass the brain, bone, spleen, lymph nodes, kidneys, pancreas and adrenal glands (12-14). In the present case, PPB manifested in the lung of a 3-year-old patient, with cough as the initial symptom.

Imaging characteristics. Imaging examinations, particularly chest CT scans, are valuable in differentiating the characteristics of lung lesions. These scans can not only identify the heterogeneity of PPB but also provide diagnostic insights into the presence of pleural effusion and chest wall invasion. For larger masses, a biopsy can be performed under CT guidance to confirm the diagnosis (15). In the present case, CT revealed a right lung mass identified as a neoplastic lesion, possibly indicative of PPB. Differentiation between neurogenic tumors and germ cell-derived tumors is necessary and should be corroborated with clinical and pathological findings. Typically, PPB presents as a solitary, well-defined mass that can exceed 10 cm (13). Based on histological variations, CT scans display different imaging characteristics. Type I PPB lesions often appear as single or multiple subpleural or intrapulmonary cystic masses, requiring differential diagnosis from other cystic lesions such as bronchogenic cysts, pulmonary cysts, pulmonary

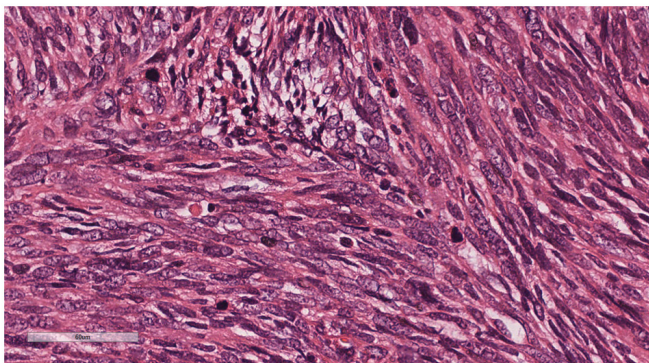


Figure 5. High-power microscopy shows that the solid portion of the tumor is composed of naive primitive embryonic components (H&E stain; magnification, x400).

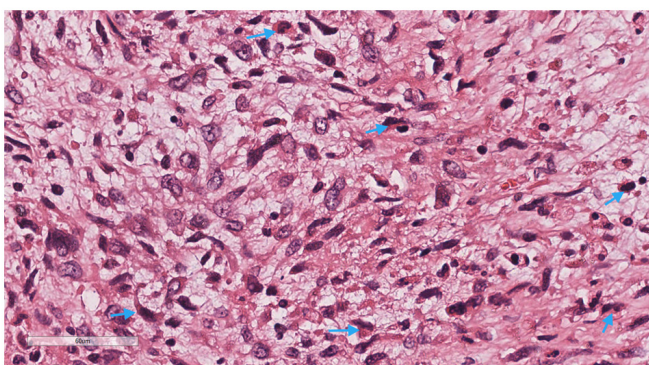


Figure 6. Microscopy reveals that the tumor cells lack malignant epithelial components, and embryonal rhabdomyosarcoma-like differentiation can be seen in certain areas (blue arrow) (H&E stain; magnification, x400).

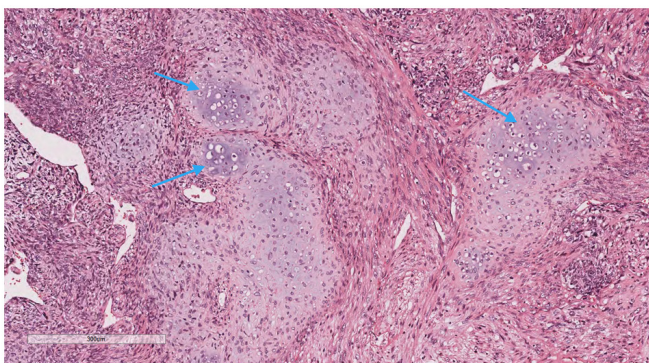


Figure 7. Immature chondrosarcomatoid differentiation can be seen in certain areas (blue arrow) of the tumor (H&E stain; magnification, x60).

bullae and interstitial emphysema. Type II PPB frequently presents as intrapulmonary cystic and solid masses, whilst type III PPB predominantly manifests as solid lesions with uniform density and clear boundaries. The differential diagnosis of type II and III PPB, especially when locally invasive, often necessitates differentiation from other malignant tumors, such as neuroblastoma, Ewing's sarcoma and rhabdomyosarcoma. Although CT provides valuable reference data for clinicians and pathologists in diagnosing PPB, it is not definitive, and the final diagnosis relies on pathological examination (3,4).

Pathological characteristics. According to the Dehner classification (14), PPB is categorized into type I (completely cystic, with a better prognosis), type II (cystic and solid) and type III (completely solid, with a poor prognosis). Certain studies further classify PPB into four types (Ir, I, II and III) based on gross pathological appearance and morphological characteristics. Type I cystic PPB may progress to invasive types II and III but may also regress to type Ir, where 'r' denotes regression, characterized by the absence of malignant tumor cells. Types II and III PPB are invasive (14,16,17). Types I and Ir exhibit a lower degree of malignancy, whereas types II and III are highly malignant and invasive. Type I PPB is typically unilateral, solitary, peripheral and >5 cm (4). Microscopically, cystic structures with fibrous septa containing immature mesenchymal cells and benign respiratory epithelium are observed. In type Ir, the cyst wall fibrous septa lack immature cells compared with type I. Type II PPB is characterized by both cystic and solid areas, with nodular solid regions containing undifferentiated ovoid and stellate cells growing in sheets, whilst the cystic areas resemble those in type I PPB. Type III is purely solid and microscopically appears as a mixture of blast cells with sarcomatous areas (chondrosarcomatous, fibrosarcomatous, rhabdomyosarcomatous and anaplastic components) present, often with frequent mitotic figures. Types II and III PPB are histologically similar in the solid areas, necessitating adequate sampling for evaluation (14,18). The immunophenotype of PPB is non-specific. Tumor cells express Vimentin and, in most cases, muscle-specific actin. Depending on differentiation, rhabdomyoblastic areas express desmin, MyoD1 and Myogenin, whilst cartilaginous areas express S-100. CK and TTF-1 mark cystic benign epithelial cells and benign epithelial cells entrapped within the tumor substance (19).

Differential diagnosis. Type III PPB must be distinguished from the following tumors: i) Classic pulmonary blastoma, which is a biphasic highly malignant tumor containing both malignant epithelial and mesenchymal components, whereas PPB comprises benign epithelial and malignant mesenchymal components. The primary distinguishing factor between the two is the presence or absence of malignant epithelial cells observed microscopically; ii) ERMS, as both ERMS and PPB exhibit concurrent mutations in Dcr-1 homolog and ribonuclease type III (DICER1), making immunohistochemistry crucial for differentiation. ERMS is a highly malignant soft tissue sarcoma originating from mesenchymal stem cells during the embryonic period, characterized by differentiation towards rhabdomyosarcoma. It presents primitive undifferentiated stellate cells, small round cells and well-differentiated cells that stain strongly with eosin, displaying tadpole-shaped, spindle-shaped, ribbon-like, tennis racket-like and large round tumor cells. ERMS shows diffuse strong expression of MyoD1 and Myogenin, whereas PPB expresses these markers focally when rhabdomyoblastic differentiation is present (19). Furthermore, a previous study reported that insulin-like growth factor is overexpressed in ERMS but under-expressed in PPB (20). Immunohistochemistry is essential for differentiating between these two entities; iii) mesenchymal chondrosarcoma (MC), a highly malignant biphasic tumor

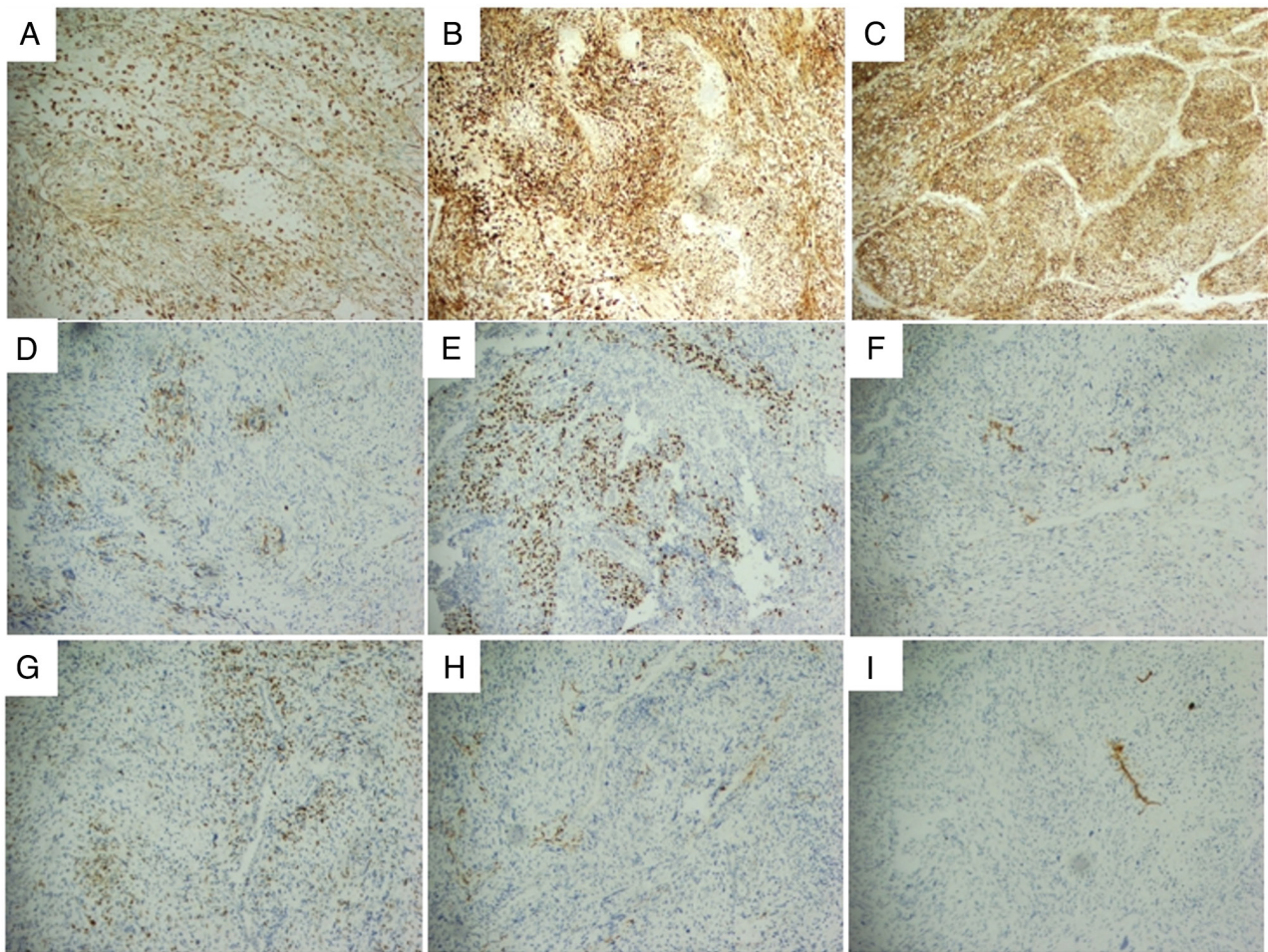


Figure 8. Immunohistochemistry results. The tumor cells exhibited positivity for (A) Vimentin, (B) CD10 and (C) CD56. (D) Desmin, (E) myogenic differentiation 1 and (F) CD99 were focally or sporadically positive. (G) Sal-like protein 4 demonstrated focal positivity, whilst (H) SMA showed local focal positivity. (I) Myogenin exhibited local scattered focal positivity (magnification, x200).

comprising undifferentiated primitive round cells and well-differentiated hyaline cartilage. The tumor cells are small to medium-sized round cells that express CD99, unlike PPB. Cartilage differentiation in MC can vary from loosely arranged small lesions to well-differentiated large areas of mature cartilage, often containing large granular calcifications. MC is characterized by the *HEY1-NCOA2* fusion gene, whereas PPB primarily exhibits heterozygous germline mutations in *DICER1* (21); iv) inflammatory myofibroblastic tumor (IMT), which the World Health Organization, in 2020, defined as a unique, rarely metastatic tumor composed of spindle-shaped myofibroblasts and fibroblasts accompanied by plasma cells, lymphocytes, eosinophils and other inflammatory cells (22). The immunophenotype of IMT expresses Vimentin and shows varying degrees of expression of SMA, calponin and desmin. A total of 50-60% of cases are ALK-positive, with about 2/3 of IMTs exhibiting ALK gene rearrangements. By contrast, PPB does not express ALK or have ALK gene rearrangements; and v) primitive neuroectodermal tumor (PNET), which is primarily composed of small round and short spindle-shaped primitive cells with diffuse distribution. Homer-Wright pseudorosettes may be observed. PNET expresses neuron-specific enolase and synaptophysin, which PPB does not express (23).

The patient in the present case had type III PPB with rhabdomyosarcoma, chondrosarcoma and other differentiations, accompanied by pleural invasion. During diagnosis, it is crucial to differentiate PPB from classic pulmonary blastoma, ERMS and MC. Moreover, differentiation should be based on clinical history, characteristic pathological morphology and immunohistochemical results.

Genetic modification. PPB and other tumors exhibit familial characteristics. Whole-exome sequencing has identified heterozygous germline mutations in *DICER1* in infants with PPB. The *DICER1* protein belongs to the ribonuclease III enzyme family (24) and the *DICER1* gene is a highly conserved gene located on chromosome 14q32.13, encoding 1,992 amino acids and comprising 27 exons. This gene controls the production of the ribonuclease enzyme, Dicer1, which serves a critical role in regulating protein translation (25). Data from the International PPB Registry indicate that ~70% of patients with PPB possess *DICER1* gene mutations (8). Common pathogenic mutations in the *DICER1* gene include loss-of-function (LOF) mutations and hotspot missense mutations in the RNase IIIb domain, with LOF mutations being the predominant mode of familial inheritance. There is a marked association between *DICER1* and

Sertoli-Leydig cell tumors (and ovarian germ cell tumors), suggesting that patients with these tumors should be tested for germline or somatic *DICER1* mutations. Thyroid nodular hyperplasia, with or without papillary thyroid carcinoma, may be the most common associated pathology in *DICER1* germline mutation carriers. Other *DICER1*-related tumors include cervical (non-vaginal) ERMS, ciliated müllerian mixed tumor, nasal chondromesenchymal hamartoma, small intestinal hamartomatous polyps and pituitary blastoma. Any of these tumors, individually or in combination, may indicate *DICER1*-related syndrome. Therefore, it is particularly important for clinicians and pathologists to raise this concern and recommend genetic counseling and testing (14). From the clinical history, typical morphology and immunohistochemical results in the present case, the diagnosis was clear; however, genetic testing was not available, which was a limitation.

Treatment and prognosis. The treatment of PPB includes surgery, chemotherapy, radiotherapy and neoadjuvant therapy. Complete surgical resection is the main goal of treatment for children with PPB. It has also been reported that neural cell adhesion molecule 1/fibroblast growth factor module can be used as a therapeutic target for pleuropulmonary blastoma (26). Type I and Ir PPB have not been reported to have metastases and are treated with complete resection with wide negative margins. Systemic chemotherapy and surgical resection are the key to the treatment of type II and type III PPB. Neoadjuvant chemotherapy after biopsy can be used for large tumors that are difficult to resect and with unpredictable negative margins. Furthermore, the prognosis of PPB is related to the pathological classification. The 5-year overall survival rate of type I and Ir PPB has been reported to be 98.0%, and that of type II and III PPB is 71 and 53%, respectively (4).

The present report describes a rare case of PPB (type III) with rhabdomyosarcoma and chondrosarcoma differentiation occurring in the middle and lower lobe of the right lung. Regular chemotherapy was performed after surgery, and the patient was followed up for 12 months. Therefore, the present report demonstrates that a comprehensive description of PPB, including clinical manifestations, imaging features, pathological features and molecular genetic changes provide a good reference value for clinical diagnosis and treatment.

PPB is the most common pulmonary malignant tumor in children, its incidence is low, it is difficult to distinguish from other lung space occupying lesions, it is difficult to diagnose early, and it often progresses into a pathological type with a poor prognosis. The disease is closely related to a *DICER1* gene variation, and children with *DICER1* syndrome and their relatives are at risk of developing multisystem tumors. The clinical manifestations of children with PPB should be paid attention to, lung imaging and pathological examinations in the early stage should be performed, as well as genetic testing if necessary and long-term monitoring of the family of a patient with *DICER1* syndrome.

Acknowledgements

Not applicable.

Funding

No funding was received.

Availability of data and materials

The data generated in the present study may be requested from the corresponding author.

Authors' contributions

SL and JW analyzed the data, conducted the histopathological evaluation and assisted in writing the manuscript. XT acquired the CT scan images. TX performed the immunohistochemical staining. XT analyzed the patient data. JJW and SL confirm the authenticity of all the raw data. All authors have read and approved the final version of the manuscript.

Ethics approval and consent to participate

The present case report was approved by the Ethics Committee of the Affiliated Hospital of Zunyi Medical University (Zunyi, China; approval no. KLLY-2024-354).

Patient consent for publication

Written informed consent was obtained from the parents of the patient for the publication of the present case report and any accompanying images.

Competing interests

The authors declare that they have no competing interests.

References

- Masarweh K, Mordechai O, Gur M, Bar-Yoseph R, Bentur L and Ilivitzki A: Challenges in *DICER1*-associated lung disease. *J Clin Med* 12: 1918, 2023.
- Nasr A, Himidan S, Pastor AC, Taylor G and Kim PC: Is congenital cystic adenomatoid malformation a premalignant lesion for pleuropulmonary blastoma? *J Pediatr Surg* 45: 1086-1089, 2010.
- Dehner LP: Pleuropulmonary blastoma is THE pulmonary blastoma of childhood. *Semin Diagn Pathol* 11: 144-151, 1994.
- Messinger YH, Stewart DR, Priest JR, Williams GM, Harris AK, Schultz KA, Yang J, Doros L, Rosenberg PS, Hill DA and Dehner LP: Pleuropulmonary blastoma: A report on 350 central pathology-confirmed pleuropulmonary blastoma cases by the International Pleuropulmonary Blastoma Registry. *Cancer* 121: 276-285, 2015.
- Hemeed H, Aly RG, Kotb M and Abdelaziz A: Pediatric pleuropulmonary blastoma: Analysis of four cases. *BMC Cancer* 24: 1268, 2024.
- Hussain M, Baig FA and Hussain S: Pulmonary blastoma. *J Coll Physicians Surg Pak* 17: 438-440, 2007.
- Bownes LV, Hutchins SC, Cardenas AM, Kelly DR and Beierle EA: Pleuropulmonary blastoma in an adolescent. *J Pediatr Surg Case Rep* 59: 101482, 2020.
- Schultz KAP, Harris AK, Nelson AT, Watson D, Lucas JT Jr, Miniati D, Stewart DR, Hagedorn KN, Mize W, Kamihara J, *et al*: Outcomes for children with type II and type III pleuropulmonary blastoma following chemotherapy: A report from the international PPB/*DICER1* registry. *J Clin Oncol* 41: 778-789, 2023.
- Gbande P, Abukeshek T, Bensari F and El-Kamel S: Pleuropulmonary blastoma, a rare entity in childhood. *Case Reports* 7: 20200206, 2021.
- Berean K, Truong LD, Dudley AW Jr and Cagle PT: Immunohistochemical characterization of pulmonary blastoma. *Am J Clin Pathol* 89: 773-777, 1988.

11. Bhalerao S, Adhav A, Gandhe S and Nagarkar R: Metachronous pleuropulmonary blastoma in an adult patient with endometrial cancer: A case report. *Oxf Med Case Reports* 2019: omz056, 2019.
12. Liu AH, Zheng WY and Wu L: Pleuropulmonary blastoma in an adult woman with pleurorrhea as the major clinical manifestation: Report of a case. *Nan Fang Yi Ke Da Xue Xue Bao* 28: 2241-2243, 2008 (In Chinese).
13. Koss MN, Hochholzer L and O'Leary T: Pulmonary blastomas. *Cancer* 67: 2368-2381, 1991.
14. Dehner LP, Messinger YH, Schultz KA, Williams GM, Wikenheiser-Brokamp K and Hill DA: Pleuropulmonary blastoma: Evolution of an entity as an entry into a familial tumor predisposition syndrome. *Pediatr Dev Pathol* 18: 504-511, 2015.
15. Engwall-Gill AJ, Chan SS, Boyd KP, Saito JM, Fallat ME, St Peter SD, Bolger-Theut S, Crotty EJ, Green JR, Hulett Bowling RL, *et al*: Accuracy of chest computed tomography in distinguishing cystic pleuropulmonary blastoma from benign congenital lung malformations in children. *JAMA Netw Open* 5: e2219814, 2022.
16. Bisogno G, Sarnacki S, Stachowicz-Stencel T, Colin VM, Ferrari A, Godzinski J, Villars MG, Bien E, Hameury F, Helfre S, *et al*: Pleuropulmonary blastoma in children and adolescents: The EXPeRT/PARTNER diagnostic and therapeutic recommendations. *Pediatr Blood Cancer* 68 (Suppl 1): e29045, 2021.
17. Landry-Truchon K, Houde N, Lhuillier M, Charron L, Hadchouel A, Delacourt C, Foulkes WD, Galmiche-Rolland L and Jeannotte L: Deletion of Yyl in mouse lung epithelium unveils molecular mechanisms governing pleuropulmonary blastoma pathogenesis. *Dis Model Mech* 13: dmm045989, 2020.
18. Knight S, Knight T, Khan A and Murphy J: Current management of pleuropulmonary blastoma: A surgical perspective. *Children* (Basel) 6: 86, 2019.
19. Han LM, Weiel JJ, Longacre TA and Folkins AK: DICER1-associated tumors in the female genital tract: Molecular basis, clinicopathologic features, and differential diagnosis. *Adv Anat Pathol* 29: 297-308, 2022.
20. Venkatramani R, Triche TJ, Wang L, Shimada H and Mascarenhas L: Insulin-like growth factor 2 gene expression molecularly differentiates pleuropulmonary blastoma and embryonal rhabdomyosarcoma. *J Pediatr Hematol Oncol* 37: e356-360, 2015.
21. Folpe A, Graham RP, Martinez A, Schembri-Wismayer D, Boland J and Fritchie KJ: Mesenchymal chondrosarcomas showing immunohistochemical evidence of rhabdomyoblastic differentiation: A potential diagnostic pitfall. *Hum Pathol* 77: 28-34, 2018.
22. Gros L, Dei Tos AP, Jones RL and Digkila A: Inflammatory myofibroblastic tumour: State of the Art. *Cancers* (Basel) 14: 3662, 2022.
23. Onoda T, Kanno M, Sato H, Takahashi N, Izumino H, Ohta H, Emura T, Katoh H, Ohizumi H, Ohtake H, *et al*: Identification of novel ALK rearrangement A2M-ALK in a neonate with fetal lung interstitial tumor. *Genes Chromosomes Cancer* 53: 865-874, 2014.
24. Dehner LP, Schultz KA and Hill DA: Pleuropulmonary blastoma: More than a lung neoplasm of childhood. *Mo Med* 116: 206-210, 2019.
25. González IA, Stewart DR, Schultz KAP, Field AP, Hill DA and Dehner LP: DICER1 tumor predisposition syndrome: An evolving story initiated with the pleuropulmonary blastoma. *Mod Pathol* 35: 4-22, 2022.
26. Shukrun R, Golan H, Caspi R, Pode-Shakked N, Pleniceanu O, Vax E, Bar-Lev DD, Pri-Chen S, Jacob-Hirsch J, Schiby G, *et al*: NCAM1/FGF module serves as a putative pleuropulmonary blastoma therapeutic target. *Oncogenesis* 8: 48, 2019.



Copyright © 2025 Luo et al. This work is licensed under a Creative Commons Attribution-NonCommercial-NoDerivatives 4.0 International (CC BY-NC-ND 4.0) License.